International Journal on Recent and Innovation Trends in Computing and Communication
ISSN: 2321-8169 Volume: 11 Issue: 2
Article Received: *25 December 2022* ***Revised:*** *12 January 2023* ***Accepted:*** *20 February 2023*

Optimization Algorithms for Combinatorial Problems: A Comparative Study of Quantum Annealing and Classical Methods

Suresh A J
Assistant Professor of Mathematics
Government Polytechnic College, Purapuzha, Thodupuzha, Idukki, Kerala
Email ID: suresh@gpcpurapuzha.ac.in
ORCID: 0009-0002-0841-2117

Abstract: Recently, a pair of quantum-annealing-inspired techniques (QAIA) have been presented for effectively resolving multimodal optimization challenges. These methods involve simulated splitting and several variations of the modelled coherently Ising device. Quantum annealing, a quantum computing paradigm, leverages quantum mechanics to explore solution spaces and promises advantages in solving certain classes of optimization problems more efficiently. Regulated evaluations between these techniques, along with other physics-based methods, are required to verify their supremacy. In this study, we compare QAIA to quantum cooling and other physics-based methods for Max-Cut issues with up to 20,000 nodes. In comparison to classical heating, we discovered that rapid modelled splitting performed exceptionally well for hybrid and tiny business graphs, delivering a time-to-solution decrease of around 50 times. If you want to find the highest cut value in Pegasus graphs, discrete simulated bifurcation works better than the D-Wave Advantage method and takes the least amount of time to reach your goal for large graphs. According to our findings, QAIA is a viable approach to practical combinatorial optimization issues and can serve as a suitable starting point for rival quantum algorithms. Finding the ideal object among a group of possibilities is known as algorithmic optimization, and it is a common problem in many fields of study, including computer science, mathematical applications, and probabilistic physics.

Keywords: Combinatorial Optimization, Quantum Annealing, Classical Optimization Methods, Traveling Salesman Problem, Graph Coloring, Heuristics, Exact Algorithms, Scalability, Performance Analysis, Hybrid Optimization Strategies.

1.Introduction:

Combinatorial optimization problems are pervasive in various domains, including operations research, artificial intelligence[1], logistics[2], and network design[3]. These problems involve finding the best solution from a finite set of possibilities, often constrained by multiple factors. Determining the best solution using traditional techniques or brute-force analysis is made extremely difficult by the "combinatorial a blast," which occurs when an issue's size increases exponentially[4]. Several heuristic methods have been developed to approximate (or discover sub-optimal) results to get around this[5-8]. However, developing an extremely precise and efficient method for solving stochastic problems remains a challenging task. The Ising issue, or determining the fundamental state of the Ising approach, can be translated to the vast bulk of optimization methods in computational physics[9-10]. A collection of N Ising rotates with an arrangement $\sigma_i = \pm 1$, a connection J_{ij} between two games, and any outside forces hi make up an Ising model. An Ising model's Hamiltonian is described as

$$I = -\frac{1}{2}\sum_{ij}^{N} jij^{\sigma} i^{\sigma} - \sum_{i}^{N} h_i\sigma_i. \qquad (1)$$

A collection of tiny bits, or qubits, can be used simply to convey this paradigm. It is generally accepted that there is no effective, accurate classical technique to address the Ising equation since it is regarded as nondeterministic polynomial time (NP) hard. To address the Ising issue, quantum machines like the D-Wave quantum annealer (QA) that uses supercharged qubits have been developed. However, experiments have shown that QA isn't good enough for processing complex graphs yet because of physical interference and limited qubit connectivity[11-14].In response to the QA, different types of machines have been made, such as the electrically powered structure, the coherent Ising machine (CIM) with pulsed lights and worsening visual linear oscillations[15–17], the memristor

International Journal on Recent and Innovation Trends in Computing and Communication
ISSN: 2321-8169 Volume: 11 Issue: 2
Article Received: *25 December 2022* ***Revised:*** *12 January 2023* ***Accepted:*** *20 February 2023*

Hopfield neural systems20, the MRAM-based unpredictable computing equipment (called P-bits)and others[21-22].

Several quantum annealing-inspired algorithms (QAIA) have been created to mimic the physical workings of classical annealing-inspired gadgets to solve computational optimization challenges. Various iterations of Simulation CIM and Simulated Bifurcation (SB) are presented in these methods. These methods employ an aging approach to enhance performance and transform individual variables into permanent ones. A system of optically adjustable oscillators is used to carry out CIM from an atomic mechanical standpoint. These oscillators display two steady states over the barrier. signifying a spin[23]. SimCIM has been used to numerically replicate CIM on conventional computers. Different iterations of CIM with adjustments for error were developed to lessen the negative consequences of reducing rotation factors. suggested, such as CIM with separated feedback control (SFC), chaotic feedback control (CFC), and chaotic volume control (CAC)[24-25]. Interestingly, all these methods simulate different versions of CIM; nonetheless, the term SimCIM refers to the specific version that was introduced in[26]. In the same way, Kerr-nonlinear dynamic oscillators used to manage classical isotherms in the quantum bifurcation machine (QbM)[27]. Conventional asymmetric Hamiltonian structures, often known as SB[28-29], simulate splitting phenomena. Adiabatic SB (aSB) is a frequent notation for the initial SB method. Errors that arise from the continuous reduction of individual variables may also impact the system. The rigid walls are then introduced by ballistic SB (bSB) to reduce analogy inaccuracies. Dynamical SB (dSB) further improves error reduction by dividing the rotation parameters within average area terms[30]. As a result, these variations produce more precise answers in addition to accelerating agreement. These methods, which were motivated by classical heating, have shown great effectiveness and precision as a viable method for resolving Ising issues. Their achievement has been documented in recent comparison studies. However, studies like only compare industrial algorithms built on systems[31-34], whereas study only looks at how various nonlinear factors affect the efficiency of digital Ising devices[35]. It is necessary to assess these quantum-inspired systems' efficiency on common hardware, such as CPUs and GPUs, to encourage and expand their use. In this study, we offer the measuring tests of QAIA and contrast them with D-Wave and a few other physics-inspired systems. Assessing their effectiveness in resolving problem areas is our aim. On the other hand, we find that QAIAs outperform the D-Wave benefit algorithm (henceforth referred to as "Benefit") in achieving the highest cut appreciation on Pegasus charts with varying issue sizes. They also achieve a shorter time-to-solution compared to heuristic computations, traditional methods, and period solutions in replica charts. In contrast, the dSB performs better overall than other QAIA standards. Especially on hybrid charts and tiny cases, the bSB demonstrates the shortest time-to-solution (TTS) and the maximum completion likelihood. For large charts, dSB demonstrates the smallest time-to-solution (TTS). On the skewed charts, however, CAC and SFC are more likely than dSB to look for the best or nearly best remedies, respectively. The inaccuracy from continual concessions without rigid walls makes the aSB vulnerable to becoming caught in regional minima. Because there are so many extreme parameters to consider, SimCIM has trouble obtaining the best results.

These methods, which were motivated by classical heating, have shown great effectiveness and precision as a viable method for resolving Ising issues. Their achievement has been documented through recent comparative research. However, studies only compare industrial solvers built on platforms, whereas study only looks at how various quadratic factors affect the accuracy of digital Ising devices. It is necessary to assess these quantum-inspired programs' efficiency on common hardware, such as CPUs and GPUs, to encourage and expand their use. In this study, we present the testing results of QAIA and compare them with D-Wave and several other physics-inspired systems. Assessing their effectiveness in resolving optimization issues is our aim. On the one hand, we discover that QAIAs surpass the benefit structure of D-Wave (henceforth referred to as "Benefit") when looking for the highest cut appreciation on Pegasus visualizations with distinct issue sizes. They additionally attain a shorter time-to-solution compared to heuristic techniques, classical, and quantity solutions in chimera visualizations. In contrast, the dSB performs better overall than other QAIA standards. Especially on chimera visualizations and small cases, the bSB demonstrates the fastest time-to-solution (TTS) and the highest success chance. For large images, dSB demonstrates the smallest time-to-solution (TTS). However, in the skewed visualizations, CAC and SFC are more likely than dSB to search for the best or nearly best remedies. The inaccuracy from repeated concessions without rigid walls makes the aSB vulnerable to becoming caught in regional minima. SimCIM struggles to achieve optimal results due to the numerous extreme parameters that need to be considered.

International Journal on Recent and Innovation Trends in Computing and Communication
ISSN: 2321-8169 Volume: 11 Issue: 2
Article Received: *25 December 2022* ***Revised:*** *12 January 2023* ***Accepted:*** *20 February 2023*

2. Literature Review

Combinatorial optimization deals with problems where the objective is to find the best solution from a finite but exponentially large set of possibilities. Typical problems include the traveling salesman problem (TSP), graph coloring, knapsack problem, and job scheduling. Due to their NP-hard nature, finding exact solutions for large instances is computationally infeasible, necessitating the use of heuristic or approximate optimization techniques.

Leleu, T et al.(2017)[1]: Driven-dissipative systems present a novel and exciting approach to combinatorial optimization, offering unique advantages such as efficient exploration of complex solution landscapes and parallel processing capabilities. While challenges remain, ongoing research and technological advancements hold significant promise for their future role in solving large-scale combinatorial problems.

Rosenberg, G. et at(2016)[2]: The optimal trading trajectory problem is a cornerstone of modern financial engineering. It seeks to determine an execution strategy that minimizes trading costs, including market impact and opportunity costs, while adhering to risk constraints. Traditional approaches, rooted in classical optimization techniques, face computational challenges as the problem's dimensionality grows. Recent advancements in quantum computing, particularly quantum annealing, offer promising avenues for solving these complex optimization problems efficiently.

Crawford, D et al(2018)[3]: Reinforcement Learning (RL) is a powerful paradigm in machine learning where agents learn optimal policies through interactions with an environment. Traditional RL approaches, while effective, encounter scalability and efficiency challenges in high-dimensional state-action spaces. Quantum computing, with its ability to process and represent large, complex data structures, offers a compelling avenue for enhancing RL. Among quantum computing frameworks, Quantum Boltzmann Machines (QBMs) have emerged as a promising tool for leveraging quantum resources in RL tasks.

Böhm, F et al.(2021)[35]: Analog Ising machines have emerged as promising candidates for solving combinatorial optimization problems, leveraging physical systems to emulate the behavior of spins in an Ising model. These machines, which include quantum annealers, optical systems, and electronic circuits, map optimization problems onto spin systems and seek their ground states. A critical factor influencing their performance is the choice of nonlinearity in their underlying physical implementation. Nonlinearity governs the energy landscape and transition dynamics of the system, directly affecting solution quality, convergence speed, and computational efficiency. This review explores the impact of nonlinearity on the computational performance of analog Ising machines, summarizing key findings from recent studies and identifying challenges and future directions.

Inc., D. et al.(2023)[48]: D-Wave's Ocean software suite is a comprehensive toolkit designed to interface with D-Wave quantum annealers and classical hybrid solvers. It provides users with tools for formulating and solving optimization problems using quantum resources, alongside integration with classical methods. The documentation accompanying the Ocean toolkit serves as a critical resource for researchers and developers, offering insights into problem formulation, solver configuration, and workflow optimization. This review examines the structure, usability, and effectiveness of the D-Wave Ocean documentation in enabling effective utilization of quantum computing resources.

Compared to other quantum computing platforms, such as IBM’s Qiskit or Rigetti’s Forest, D-Wave’s Ocean documentation stands out for its application-focused approach. While Qiskit emphasizes quantum circuit programming and Rigetti provides tools for gate-based quantum computing, Ocean’s strength lies in its specialized focus on optimization problems and quantum annealing. However, Qiskit’s documentation offers more extensive community resources, such as forums and user-contributed tutorials, which Ocean lacks. Rigetti’s emphasis on hardware-specific details also contrasts with Ocean’s abstraction layers that simplify problem-solving.

3.Methods

We test two types of annealing-inspired techniques—simulating CIM and SB—along with some extra physics-based calculations, like NMFA and TTN, on spin-glass and Max-Cut problems in this work.

3.1 The algorithms are influenced by quantum cooling

Coherent Ising Machine Simulation. Each cycle of SimCIM replicates one optical pulse roundtrip across the fiber network. Every pulse's real intensity can be used to describe the CIM's functioning as c-number randomized differential calculations[36-45]. Random simultaneous equations can be

International Journal on Recent and Innovation Trends in Computing and Communication
ISSN: 2321-8169 Volume: 11 Issue: 2
Article Received: *25 December 2022* ***Revised:*** *12 January 2023* ***Accepted:*** *20 February 2023*

used to describe the optical heartbeat, optical pressing, nonlinear and linear loss, and cacophony of CIM. To simplify calculation, SimCIM removes the fictitious component of the waveform and the chaotic part. SimCIM then continuously updates the spin parameters, A= {Ai}, as shown below.

$$\frac{P_{xi}}{dt} = \left(vA_i + \zeta \sum_j j_{ij} A_j\right) + \sigma f_i, \qquad (2)$$

where fi is a Gaussian noise, v stands for the variable increase and the linear loss parameters, and ζ is the pairing intensity. To guarantee that the final goal function is equal to the Hamiltonian of the Ising issue, v progressively rises to zero through optimization. Slope descent with velocity is the method used to solve this issue of optimization[45-56]. Frequency variability in the typical CIM results in an incorrect connection to the power value. An auxiliary constant e_I, often known as the error factor, is added for mistake discovery and repair to get around this. The spin parameter and mistake parameter's time evolution can be explained as below.

$$\frac{P_{Ai}}{Pt} = -A_i^3 + (s-1)A_i + e_i \sum_j \zeta j_{ij} A_j, \qquad (3)$$

$$\frac{P_{ei}}{Pt} = -\beta_{ei}(A_i^2 - \sigma), \qquad (4)$$

where s, α, and β stand for the goal amplitude, the increase dimension, and the pace at which the mistake parameters shift, respectively. Fault factors expedite the resolution of the Ising issue by inducing erratic behaviours in the structure, leading to the investigation of successive setups near its original state. CAC is the name given to this technology. The main difference between CAC and CFC, another variation of Virtual CIM, is that the time development of the error parameter is controlled by the output signal x_i, not the amplitude A_i.

$$x_i = -e_i \sum_j \zeta j_{ij} A_j, \qquad (5)$$

$$\frac{P_{Ai}}{Pt} = -A_i^3 + (s-1)A_i + x_i \qquad (6)$$

$$\frac{P_{ei}}{Pt} = -\beta_{ei}(x_i^2 - \alpha), \qquad (7)$$

SFC separates the error factor and the dependent variable into two linear concepts as opposed to the nonlinear variables associated with these two components, like CAC and CFC do.

$$x_i = -\sum_j \zeta j_{ij} A_j, \qquad (8)$$

$$\frac{P_{Ai}}{Pt} = -A_i^3 + (s-1)A_i \ \tanh(cx_i) - k(x_i - e_i) \qquad (9)$$

$$\frac{P_{ei}}{Pt} = -\beta_{ei}(e_i - x_i), \qquad (10)$$

The system variables in this case are p, k, c, and by adjusting the parameters, the tanh equation solves the amplitude diversity issue. The local minimum traps are destabilized due to the discrepancy between the error parameter and the feedback message. Every CIM may encounter an environment that requires error repair. It bears a striking resemblance to the aSB, as illustrated in Supplementary Fig. 1. Nevertheless, these variations converge more quickly than the initial SB and SimCIM with the aid of corrections for mistakes (Fig. 2).

Simulated Bifurcation (SB). QbM tries to solve the Ising problem by simulating the Kerr asymmetric oscillators, which create a quantum mix of two oscillation contents [50–54]. The traditional mechanical Hamiltonian formulates aSB this way to effectively replicate huge-scale QbM in modern digital machines:

$$\frac{P_{Ai}}{Pt} = a_0 y_i, \qquad (11)$$

$$\frac{P_{yi}}{Pt} = -(x_i^2 + a_0 - a(t))_{xi} + c_0 \sum_{j=1}^{M} j_{ij} x_j, \qquad (12)$$

where c0 indicates the binding power, J_{ij} is the linking parameter of the Ising issue without an outside magnetic field in (1), a_0 is the positive detuning rate, and a(t) is the time-varying transporting amplitude boosting from zero. X_i and Y_i represent the acceleration and position of the i^{th} Kerr-nonlinear adaptive oscillator, respectively. We add the completely inelastic barriers at $(x_i) = \pm 1$ in the bSB. X_i is changed to for every iteration, and y_i is set to 0 if $|x_i| > 1$. Such barriers force locations to be precisely equivalent to 1 or -1 when a(t) grows to a large enough value. Additionally, V_{aSB} eliminates the fourth-order part, as rigid walls may function similarly to curvilinear potential barriers. The formulae of motion are provided accordingly.

$$\frac{P_{Ai}}{Pt} = a_0 y_i, \qquad (13)$$

$$\frac{P_{yi}}{Pt} = -(x_i^2 + a_0 - a(t))_{xi} + c_0 \sum_{j=1}^{M} j_{ij} x_j, \qquad (14)$$

When t is sufficiently small, the start point in the aSB of the two spin instances becomes the single minimal point. After the initial division, two saddles emerge close to the base, and that point becomes a saddle as a(t) increases. The saddle

International Journal on Recent and Innovation Trends in Computing and Communication
ISSN: 2321-8169 Volume: 11 Issue: 2
Article Received: *25 December 2022* ***Revised:*** *12 January 2023* ***Accepted:*** *20 February 2023*

where the two regional minima occur is revealed to be the source of the bSB.[1, 1] and [−1, −1]. Consequently, there is an acceleration of closure (Fig. 2). To further reduce the constant repose mistake, the bSB can be further developed by dSB, whose movement formulas are provided by

$$\frac{P_{Ai}}{Pt} = a_0 y_i, \quad (15)$$

$$\frac{P_{yi}}{Pt} = - (x_i^2 + a_0 - a(t))_{xi} + c_0 \sum_{j=1}^{M} j_{ij}\, sgn(x_j), \quad (16)$$

Specifically, in Eq. (15), it is separated by assigning$\sum_{j=1}^{M} j_{iA} A_i A_j, \sum_{j=1}^{M} j_{ij} A_i (A_i)$. Unlike aSB and bSB, dSB examines a large range of answers at the start of the repetition, allowing it to bounce out of regional limits to accomplish more rapid convergence.

3.2 The algorithms based on physics

Because of its exceptional scalability, NMFA is utilized for evaluation in every trial, whereas TTN only offers the best trim result in the final test.

3.2.1 Noisy Mean Field Annealing (NMFA). The core step of CIM is the integration of mean-field calculation55 and spin gauges, which is carried out by the traditional FPGA coprocessor. A traditional computer is used in NMFA to carry out the remaining optical component of CIM. So, mean-field heating lowers the Hamiltonian. A Gaussian signal is added to avoid regional minimums, and the individual spin numbers are changed to smooth integers in the range [-1, 1]. The spin number can then be updated in the manner described below.

$$A_i^{\wedge} = \tanh\left[\left(\sum_j j_{ij} A_j \sqrt{\sum_j j_{ij}^2 + M\ (0, \sigma}\right) / D_t\right] \quad (17)$$

$$A_i = \alpha_{Ai}^{\wedge} + (1 - \alpha)_{Ai} \quad (18)$$

The variable α functions as the slope technique's velocity to speed up convergence, Tt represents the temperature level that steadily drops during cooling, and σ represents the noise amplitude.

3.2.2 Tropical Tensor Network (TTN). The tensor network shrinkage may give the exact base state power and entropy of the simulation at zero humidity when combined with the tropical alphabet formed on the semiring of (R ∪ {-∝},∫, ⊙) operations represent[56].

$$A \int B = \max(A, B), \quad A \int B = A + B. \quad (19)$$

The ideal spin arrangement is chosen by ⊕ during the expansion, and the power from the tensor network's subsections is added by ⊙. To sample the base state configuration [57], the TNN compression is carried out differentially at the exact time. Without listing the responses, the basic state defects can be obtained by combining the typical algebra with the tropical algebra[58].

4. Experimental setup

Every algorithm has a variety of variable types. Each method has a variable that governs the method of annealing, like the pump-loss factor v in SimCIM, the circulating amplitude a(t) in SB, and the temp. T in NMFA. This value increases exponentially in SB and NMFA. Just two of the four regional minima in the SimCIM environment match the minimizer of the Ising issue, as can be shown from the prospective power environment (Fig. 1). To prevent the value from becoming stuck in a regional minimum at the start of the iterations, we raise the flow loss factor using a hyperbolic tangent value instead of a linear value. The acceleration in SimCIM is set to β = 0.9 for the same purpose. The rate of positive adjusting in SB is set at $a_0 = 1$. Reaching an approximate answer can be accelerated by setting $a_0 = 1. c_0 = \frac{a_0}{\lambda_{max}}$ $(\lambda_{max})$is the greatest eigenvalue of the linking matrix J = $\left(j_{ij}\right)_{m\times m}$). According to Wigner's semicircle law[59-62], the calculation of λ_{max} for weighted Max-Cut and spin-glass issues is $2\sqrt{N}\sqrt{\frac{\sum_{ij} j2}{M(M-1)}}$.

The value for unweighted Max-Cut situations with $J_{ij} \in \{0, 1\}$ is λ_{max} ¼ maxi P j J_{ij} . The paper specifies how the settings of the CIMs with fixing mistakes are established. Grid search is used to determine the remaining variables for each technique, and Supplementary Tables 1–2 display the parameters for the various methods.

5. Results and discussion

We conduct numerical tests on three distinct databases and assess the algorithm's efficiency using failure likelihood and time-to-target (TTT). Before presenting the findings of the quantitative tests, we provide a brief explanation of the spin-glass, Max-Cut, and TTS/TTT challenges. Issues with Spin-Glass and Max-Cut the Ising structures with Gaussian-distributed fittings between nearby spins are described by the spin-glass theory. The spin-glass issue involves determining the base state of the Ising move glass using the

International Journal on Recent and Innovation Trends in Computing and Communication
ISSN: 2321-8169 Volume: 11 Issue: 2
Article Received: *25 December 2022* ***Revised:*** *12 January 2023* ***Accepted:*** *20 February 2023*

power value Equation (1). The Max-Cut issue bears resemblance to the task of reducing the Hamiltonian of a turn glass model in mathematical physics and in disturbed structures. One of the significant multimodal optimization issues is the Max-Cut problem. Let T = (V, E) be an undirected graph with edge weights $w_{ij} = w_{ji} > 0$ for all (i, j) ∈ E and |V| = M. To increase the total of the weighted borders linking the locations in these two distinct parts, we divide the vertices V into two supplementary groups. The scaled Max-Cut can have any infinite or negative weight numbers, whereas the Max-Cut only has +1 weights. To illustrate the two categories, we first give each network node an Ising spin $\sigma_i \in \{-1, 1\}$, which can be described as the Ising issue. Thus, it may be expressed as follows:

$$\text{Arg max} \sum_{(i,j)\epsilon E} w_{ij}(1 - \sigma_1\sigma_j)$$

$$= \frac{1}{2} \sum_{ij}^{M} jij^{\sigma} i^{\sigma} + \sum_{(i,j)\epsilon E} w_{ij} \qquad (20)$$

The expression can be expressed as follows: Keep in mind that the next term, $\sum_{ij} w_{ij}$, is an integer, and the Hamiltonian H in Eq. (1) with the zero outside force is equal to increasing the initial part in (2). We select the Max-Cut issue (2) for evaluating since it easily transfers onto the Ising issue (1).

5.1 The metrics used for evaluation

The QAIA methods are all heuristic. To thoroughly evaluate various approaches, we calculate the achievement chance P—the ratio of reaching the ideal solution—by sampling every visualization 100 times. In the meantime, the method's computing speed is evaluated using TTS and TTT. TTT calculates how long it takes the method to ensure that the original result can happen more than once with a likelihood Q that is typically set at 0.99. The likelihood of obtaining the needed solution when executing a stochastic solver for a duration Ts is $P(T_s)$. Think about the scenario of k trials; the likelihood of getting at least one right outcome is provided by

$$Q = 1 - (1 - P(T_s))^k; \qquad (22)$$

then the number of operations required to accomplish the just result with a chance of Q (= 0.99) is given by k =

$$\frac{log(1 - 0.99)}{(1 - P(Ts))} \text{ TTT}$$

$$= \begin{cases} D_s \log(1 - 0.99) / \log(1 - P(D_s)); D_s < 0{:}99; \\ D_s; P(D_s) \geq 0.99; \end{cases}$$

(23)

where Ts is the time to run the algorithm once. P (D_s) is set to the success chance P for TTS. Additionally, in TTT, the baseline goal is typically defined as 99% of the most well-known or accurate figure. Furthermore, we calculate the RMedian and Rmax, or mean and highest, of the proportion between the test's cut result and the ideal one.

5.2 First Experiment

We evaluate QAIA on tiny normal visualizations in the initial test, with problem sizes N varying from 10 to 500. We chose the scale to {−1, 1} because we need to see a pattern of QAIA efficiency on normal visualizations with a bigger issue size. Based on the edge mass and volume, the issues can be categorized into four groups, such as weak and deep spin-glass examples and weak and deep Max-Cut cases[36]. For every challenge, we generate 10 instances of each size to determine the median efficiency. These examples are produced using the Python module Network, and the Biq Max solver, an exact technique that uses semidefinite coding based on the Fork & Limit method, has already determined the cut number of the visualizations[37-38]. In each case, the parameters are assessed on QAIAs for 10,000 repetitions to improve the test findings' dependability. Various methods exhibit notable differences in performance under thin situations. Compared to previous methods, the bSB significantly improves both the success chance and TTS. It also exhibits greater durability as the issue size increases, irrespective of whether it is applied to Max-Cut examples (Fig. 1) or spin-glass examples (Fig. 2). The performance of SimCIM, aSB, and dSB is comparable. Additionally, the SimCIM yields a lower TTS, while the dSB achieves a slightly higher resilience and outcome chance. In this trial, they outperform the NMFA. However, QAIA's efficiency often equals that of large visualizations. The article is: https://doi.org/10.1038/s42005-0.

International Journal on Recent and Innovation Trends in Computing and Communication
ISSN: 2321-8169 Volume: 11 Issue: 2
Article Received: *25 December 2022* ***Revised:*** *12 January 2023* ***Accepted:*** *20 February 2023*

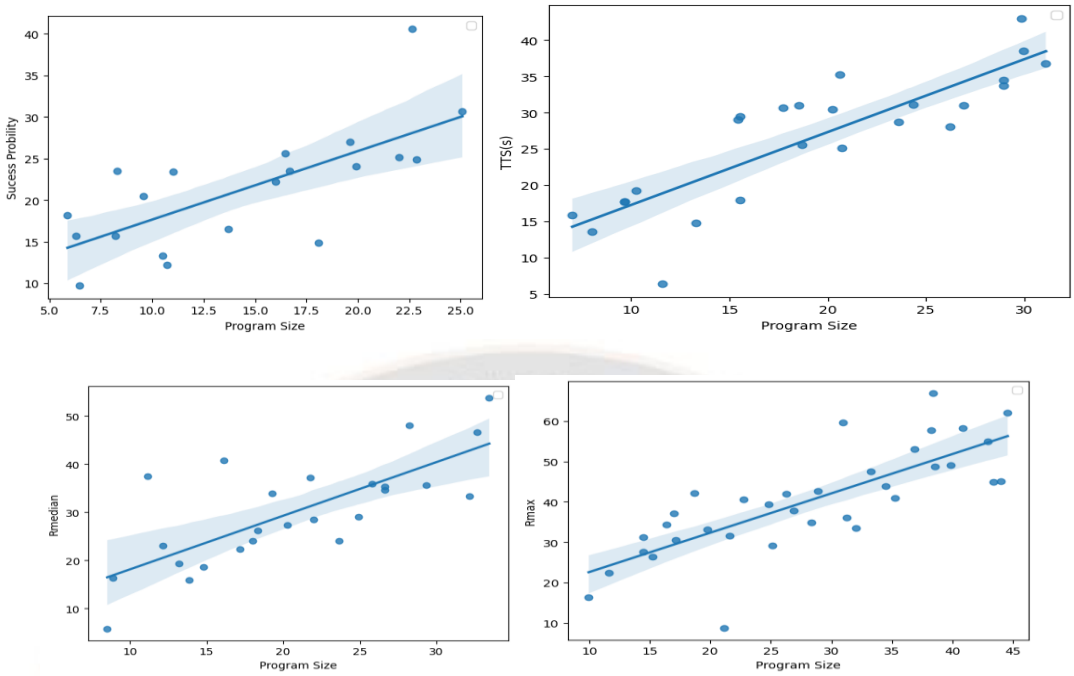

Figure 1 illustrates the QAIA comparison results for 3-regular Max-Cut problems on GPUs with high weights. Victory Chance, Time-to-Solution (TTS), and the average and highest of the ratios between the specimen's cut number and the ideal cut number, Rmedian and Rmax, respectively, are presented in (a) Victory Chance and (b) Time-to-Solution (TTS). Every use of the methods undergoes 1,000 rounds over 10,000 trials. The solid arcs in (a) and (b), which illustrate the trend of the parameters as the issue size grows, are obtained by matching the matching information points for each technique.

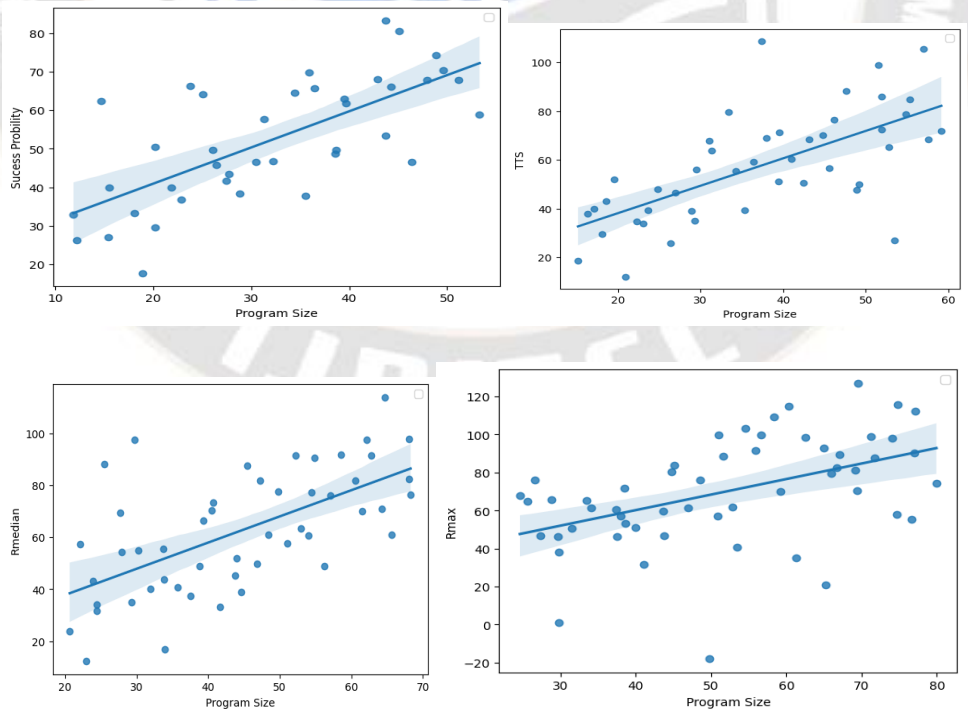

Figure 2: Quantum cooling influences the evaluation of techniques for three typical spin glass issues on a GPU. The first three variables are Achievement Chance, Time-to-solution (TTS), and the average and highest ratios between the test's cut level and the

International Journal on Recent and Innovation Trends in Computing and Communication
ISSN: 2321-8169 Volume: 11 Issue: 2
Article Received: *25 December 2022* ***Revised:*** *12 January 2023* ***Accepted:*** *20 February 2023*

ideal cut level (Rmedian and Rmax, respectively). Every use of the methods involves 1,000 rounds over 10,000 sessions. The solid arcs in (a) and (b) illustrate the trend of the measures and the growth in issue size, respectively, when the matching information points for each method are matched.

5.3 Second Experiment

The final one compares QAIA to QA with the most powerful processing power using the chimera and pegasus charts of the real D-Wave gadget11,43. The Tropical Tensor Network (TTN)44 offers the base state efficiency of the spin-glass example, enabling chimera visualizations. We contrast QAIA with a few exact solutions from the published works of QA and other physics-based algorithms [13, 45]. Figure 3 illustrates how bSB achieves this.

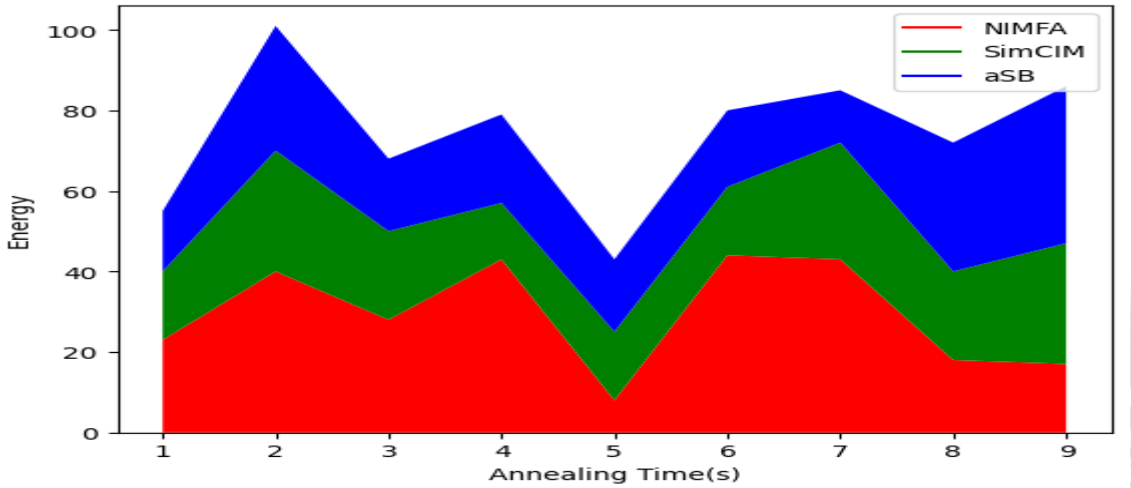

Figure 3: Ising energy development. G22 is a sparse chart; K2000 is a dense graph. One CPU core is used for both simulated annealing (SA) and methods influenced by quantum melting. The max and min instances among the 100 trials are represented by dashed lines, while the solid lines show the mean power.

Table 1 We are comparing the spin-glass power values with the chimera visualizations.

Time(s)	Algorithm	Hardware	Graph size
<0.64	dsb	GPU tesla v100	
17.63	dsb	CPU 1 crore	
~2886	Extract belief propagation[13]	CPU 1 crore	
$>10^{108}$	Brute force search[48]	G titan V	8× 8 × 8
83	TTN[44]	GPU tesla v100	
32600	TTN	CPU 1 crore	

International Journal on Recent and Innovation Trends in Computing and Communication
ISSN: 2321-8169 Volume: 11 Issue: 2
Article Received: *25 December 2022* ***Revised:*** *12 January 2023* ***Accepted:*** *20 February 2023*

<0.007	Bsb	GPU tesla v100	
0.14	Bsb	CPU 1 crore	
~0.07	QA[13]	D wave	
~0.97	Extract belief propagation[13]	CPU 1 crore	$4 \times 4 \times 8$
$>10^{47}$	Brute force search[48]	G titan V	
5.63	TTN	CPU 1 crore	

in this document. Consequently, QAIA provides a useful starting point for developing rival quantum methods.

Table 2 The performance evaluation of methods is influenced by quantum heating.

SFC	**aSB**	**bSB**	**NMFA**	**SiMCiM**	**dSB**	**CAC**	**CFC**	**Metric**	**Class of graph**
5.8	5	3.6	5.83	3.85	4	4.98	6		Average ranking
5	7	1	4	3	4	8	6	TTT	
4	7	1	3	3	4	2	6	98% of best	
5	7	2	4	2	3	2	5	P	Large dense (N>2000)
3	7	3	4	1	1	6	5	TTT	
6	4	3	4	4	3	5	4	98% of best	
4	5	3	6	4	2	6	4	P	Large/skew (N = 2000)

International Journal on Recent and Innovation Trends in Computing and Communication
ISSN: 2321-8169 Volume: 11 Issue: 2
Article Received: *25 December 2022* ***Revised:*** *12 January 2023* ***Accepted:*** *20 February 2023*

8	4	5	6	4	3	6	3	TTT	
8	3	5	7	2	4	8	3	98% of best	
8	3	4	5	2	5	-	-	P	Large/random (N ≥ 2000)
6	3	4	5	2	5	-	-	TTS	
4	3	4	5	4	3	-	-	P	Small/dense
3	8	4	1	4	4	-	-	TTS	
5	8	1	2	1	3	7	4	P	Small/sparse
6	8	1	2	1	3	8	3	TTS	
5	7	1	2	5	3	8	3	P	Pegasus
5	7	5	2	5	3	8	6	98% of best	
8	7	5	5	4	4	9	5	P	Chimera

6. Conclusions

In this study, we evaluated quantum-inspired methods that addressed the factorial issue on a variety of network types. We also compared these methods with the D-Wave quantum annealer and a few physics-based techniques. In the summary of the testing findings. Not only does bSB perform exceptionally well in chimera charts when compared to other QAIAs, but it also offers a remarkable TTS decrease of around 50 times when compared to D-Wave. Overall, CAC performs better than other options for Pegasus graphs. Furthermore, unlike the benefit structure of D-Wave crashes, CFC and dSB can search for optimal solutions across a wide range of issue sizes' continuously exhibits greater accuracy on tiny visualizations. The problem's solution likelihood and TTT remain unchanged as its scope increases. Large, random, skewed, and thick graphs are best suited for CAC, CFC, and dSB, which have the greatest success chances and the shortest TTT, respectively. The properties of the charts involved determine which solver is best for addressing optimization issues. For chimera and tiny graphs, bSB is the optimal choice. Nevertheless, dSB turns out to be the best solution for bigger graphs. However, for big stochastic and skewed visualizations, CAC and SFC could work better than dSB given enough time and computer resources since they have a larger chance of producing ideal or nearly perfect solutions. SimCIM and aSB are included in the initial version of QAIA, which is prone to becoming trapped in local minima . However, QAIA shows a notable boost in efficiency when outfitted with separation, error mitigation, or rigid walls. Interestingly, QAIA outperforms the D-wave annealer and other traditional algorithms in discovering the best options quickly.

References

1. Leleu, T., Yamamoto, Y., Utsunomiya, S. & Aihara, K. Combinatorial optimization using dynamical phase transitions in driven-dissipative systems. Physical Review E 95, 022118 (2017).
2. Rosenberg, G. et al. Solving the optimal trading trajectory problem using a quantum annealer. IEEE Journal of Selected Topics in Signal Processing 10, 1053–1060 (2016).
3. Crawford, D., Levit, A., Ghadermarzy, N., Oberoi, J. S. & Ronagh, P. Reinforcement learning using quantum boltzmann machines. Quantum Inf. Comput. 18, 51–74 (2018).
4. Siarry, P.Metaheuristics (Springer, 2016). 5. Arora, S. & Barak, B.Computational Complexity - A Modern Approach (Cambridge University Press, 2009).
6. Kirkpatrick, S., Gelatt, C. D. & Vecchi, M. P. Optimization by simulated annealing. science 220, 671–680 (1983).
7. Bilbro, G. L. et al. Optimization by mean field annealing. In Touretzky, D. S. (ed.) Advances in Neural Information Processing Systems 1, [NIPS Conference, Denver, Colorado, USA, 1988], 91–98 (Morgan
Kaufmann, 1988).
8. Goemans, M. X. & Williamson, D. P. Improved approximation algorithms for maximum cut and satisfiability problems using semidefinite programming. JACM 42, 1115–1145 (1995).
9. Smith, K. A. Neural networks for combinatorial optimization: a review of more than a decade of research. INFORMS J. Comput. 11, 15–34 (1999).
10. Lucas, A. Ising formulations of many np problems. Front. Phys. 2, 5 (2014).
11. Johnson, M. W. et al. Quantum annealing with manufactured spins.Nature 473, 194–198 (2011).
12. Bunyk, P. I. et al. Architectural considerations in the design of a superconducting quantum annealing processor. IEEE Transactions on Applied Superconductivity 24, 1–10 (2014).
13. Boixo, S. et al. Evidence for quantum annealing with more than one hundred qubits. Nature physics 10, 218–224 (2014).
14. Boev, A. S. et al. Quantum-inspired optimization for wavelength assignment. Frontiers in Physics 10, 1092065 (2023).
15. Marandi, A., Wang, Z., Takata, K., Byer, R. L. & Yamamoto, Y. Network of time-multiplexed optical parametric oscillators as a coherent ising machine. Nature Photonics 8, 937–942 (2014).
16. Inagaki, T. et al. A coherent ising machine for 2000-node optimization problems. Science 354, 603–606 (2016).
17. McMahon, P. L. et al. A fully programmable 100-spin coherent ising machine with all-to-all connections. Science 354, 614–617 (2016).
18. Mahboob, I., Okamoto, H. & Yamaguchi, H. An electromechanical ising hamiltonian. Science advances 2, e1600236 (2016).
19. Aramon, M. et al. Physics-inspired optimization for quadratic unconstrained problems using a digital annealer. Frontiers in Physics 7, 48 (2019).
20. Cai, F. et al. Power-efficient combinatorial optimization using intrinsic noise in memristor hopfield neural networks. Nature Electronics 3, 409–418 (2020).
21. Camsari, K. Y., Sutton, B. M. & Datta, S. P-bits for probabilistic spin logic. Applied Physics Reviews 6, 011305 (2019).
22. Borders, W. A. et al. Integer factorization using stochastic magnetic tunnel junctions. Nature 573, 390–393 (2019).
23. Wang, Z., Marandi, A., Wen, K., Byer, R. L. & Yamamoto, Y. Coherent ising machine based on degenerate optical parametric oscillators. Physical Review A 88, 063853 (2013).
24. Reifenstein, S., Kako, S., Khoyratee, F., Leleu, T. & Yamamoto, Y. Coherent ising machines with optical error correction circuits. Advanced Quantum Technologies 4, 2100077 (2021).
25. Reifenstein, S. et al. Coherent sat solvers: a tutorial. Advances in Optics and Photonics 15, 385–441 (2023).
26. Tiunov, E. S., Ulanov, A. E. & Lvovsky, A. Annealing by simulating the coherent ising machine. Optics express 27, 10288–10295 (2019).
27. Goto, H. Bifurcation-based adiabatic quantum computation with a nonlinear oscillator network. Scientific reports 6, 1–8 (2016).
28. Goto, H., Tatsumura, K. & Dixon, A. R. Combinatorial optimization by simulating adiabatic bifurcations in nonlinear hamiltonian systems. Science advances 5, eaav2372 (2019).
29. Goto, H. et al. High-performance combinatorial optimization based on classical mechanics. Science Advances 7, eabe7953 (2021).
30. Wang, J., Ebler, D., Wong, K. M., Hui, D. S. W. & Sun, J. Bifurcation behaviors shape how continuous

physical dynamics solves discrete ising optimization. Nature Communications 14, 2510 (2023).

31. Oshiyama, H. & Ohzeki, M. Benchmark of quantum-inspired heuristic solvers for quadratic unconstrained binary optimization. Scientific reports 12, 2146 (2022).
32. Kowalsky, M., Albash, T., Hen, I. & Lidar, D. A. 3-regular threexorsat planted solutions benchmark of classical and quantum heuristic optimizers. Quantum Science and Technology 7, 025008 (2022).
33. Jiang, J.-R. & Chu, C.-W. Classifying and benchmarking quantum annealing algorithms based on quadratic unconstrained binary optimization for solving np-hard problems. IEEE Access (2023).
34. Mohseni, N., McMahon, P. L. & Byrnes, T. Ising machines as hardware solvers of combinatorial optimization problems. Nature Reviews Physics 4, 363–379 (2022).
35. Böhm, F., Van Vaerenbergh, T., Verschaffelt, G. & Van der Sande, G. Order-of-magnitude differences in computational performance of analog ising machines induced by the choice of nonlinearity. Communications Physics 4, 1–11 (2021).
36. Barahona, F., Grötschel, M., Jünger, M. & Reinelt, G. An application of combinatorial optimization to statistical physics and circuit layout design. Operations Research 36, 493–513 (1988).
37. Schult, D. A. & Swart, P. Exploring network structure, dynamics, and function using networkx. In Proceedings of the 7th Python in science conferences (SciPy 2008), vol. 2008, 11–16 (Pasadena, CA, 2008).
38. Rendl, F., Rinaldi, G. & Wiegele, A. Solving Max-Cut to optimality by intersecting semidefinite and polyhedral relaxations. Math. Programming 121, 307 (2010).
39. Benlic, U. & Hao, J.-K. Breakout local search for the max-cutproblem. Engineering Applications of Artificial Intelligence 26, 1162–1173 (2013).
40. Isakov, S. V., Zintchenko, I. N., Rønnow, T. F. & Troyer, M. Optimised simulated annealing for ising spin glasses. Computer Physics Communications 192, 265–271 (2015).
41. Inc., J.https://github.com/OpenJij/OpenJij (2019).
42. Inc., D.-W. S.https://github.com/dwavesystems/dwave-neal (2017).
43. McGeoch, F. P., C. The d-wave advantage system: an overview. Tech. Rep., D-Wave Systems Inc, Burnaby, BC, Canada (2020).
44. Liu, J.-G., Wang, L. & Zhang, P. Tropical tensor network for ground states of spin glasses. Physical Review Letters 126, 090506 (2021).
45. Dechter, R. Bucket elimination: A unifying framework for reasoning. Artificial Intelligence 113, 41–85 (1999).
46. Jałowiecki, K., Rams, M. M. & Gardas, B. Brute-forcing spin-glass problems with cuda. Computer Physics Communications 260, 107728 (2021).
47. Huang, T. et al. Benchmarking quantum (-inspired) annealing hardware on practical use cases. IEEE Transactions on Computers 72, 1692–1705 (2022).
48. Inc., D.-W. S. D-wave ocean documentation: Dnx generators (2021). https://docs.ocean.dwavesys.com/projects/dwave-networkx/en/ latest. Accessed on September 27, 2023.
49. Kanao, T. & Goto, H. Simulated bifurcation assisted by thermal fluctuation. Communications Physics 5, 153 (2022).
50. Goto, H. Bifurcation-based adiabatic quantum computation with a nonlinear oscillator network. Scientific reports 6, 21686 (2016).
51. Nigg, S. E., Lörch, N. & Tiwari, R. P. Robust quantum optimizer with full connectivity. Science advances 3, e1602273 (2017).
52. Puri, S., Andersen, C. K., Grimsmo, A. L. & Blais, A. Quantum annealing with all-to-all connected nonlinear oscillators. Nature communications 8, 1–9 (2017).
53. Goto, H., Lin, Z. & Nakamura, Y. Boltzmann sampling from the ising model using quantum heating of coupled nonlinear oscillators. Scientific reports 8, 1–9 (2018).
54. Goto, H. Quantum computation based on quantum adiabatic bifurcations of kerr-nonlinear parametric oscillators. Journal of the Physical Society of Japan 88, 061015 (2019).
55. King, A. D., Bernoudy, W., King, J., Berkley, A. J. & Lanting, T. Emulating the coherent ising machine with a mean-field algorithm. arXiv preprint arXiv:1806.08422 (2018). https://arxiv.org/abs/ 1806.08422.
56. Maclagan, D. & Sturmfels, B. Introduction to tropical geometry. Graduate Studies in Mathematics 161, 75–91 (2009).
57. Liao, H.-J., Liu, J.-G., Wang, L. & Xiang, T. Differentiable programming tensor networks. Physical Review X 9, 031041 (2019).

58. Zhang, P., Zeng, Y. & Zhou, H. Stability analysis on the finitetemperature replica-symmetric and first-step replica-symmetrybroken cavity solutions of the random vertex cover problem. Physical Review E 80, 021122 (2009).
59. Arnold, L. On wigner's semicircle law for the eigenvalues of random matrices. Zeitschrift für Wahrscheinlichkeitstheorie und verwandte Gebiete 19, 191–198 (1971).
60. Alon, N., Krivelevich, M. & Vu, V. H. On the concentration of eigenvalues of random symmetric matrices. Israel Journal of Mathematics 131, 259–267 (2002).
61. Nosal, E.Eigenvalues of graphs. Master's thesis, University of Calgary (1970).
62. Bergstra, J. & Bengio, Y. Random search for hyper-parameter optimization. J. Mach. Learn. Res. 13, 281–305 (2012).